RSC Advances

PAPER

View Article Online
View Journal | View Issue



Cite this: *RSC Adv.*, 2015, **5**, 62336

# Low band-gap polymers based on easily synthesized thioester-substituted thieno[3,4-*b*] thiophene for polymer solar cells

Dangqiang Zhu,[ab] Liang Sun,[a] Xichang Bao,[a] Shuguang Wen,[a] Liangliang Han,[a] Chuantao Gu,[ab] Jing Guo[a] and Renqiang Yang*[ac]

Received 8th July 2015
Accepted 13th July 2015

DOI: 10.1039/c5ra13381e

www.rsc.org/advances

A new acceptor *S*-alkyl thieno[3,4-*b*]thiophene-2-carbothioate-based acceptor (TTS) was firstly developed *via* easy of synthesis and applied in the construction of donor–acceptor (D–A) type conjugated polymers, by replacing the alkyl chain of ketone-substituted thieno[3,4-*b*]thiophene with an alkylthio side chain. Then, two new TTS-based polymers PBDTT-TTSO and PBDTT-TTSE were synthesized by Stille coupling reaction. The TTS acceptor moieties made the polymers exhibit a lower band gap (~1.5 eV) and appropriate HOMO and LUMO energy levels relative to the fullerene acceptors, which could make the polymers perform well in photovoltaic devices. Solar cells were fabricated with the structure ITO/PEDOT:PSS/polymer:$PC_{71}BM$/Ca/Al. The polymer PBDTT-TTSO device exhibits a power conversion efficiency (PCE) of 4.7% with an open circuit voltage ($V_{OC}$) of 0.68 V, a short circuit current density ($J_{SC}$) of 12.7 mA $cm^{-2}$, and a fill factor (FF) of 54.6% while the PBDTT-TTSE device yields a higher PCE of 5.8% with a $V_{OC}$ of 0.70 V, a $J_{SC}$ of 14.6 mA $cm^{-2}$, and a FF of 56.7%. The results indicate that thioester-substituted thieno[3,4-*b*]thiophene (TTS) is a promising building block for further design of high performance photovoltaic polymers.



## Introduction

Polymer solar cells (PSCs) have attracted much attention because of their potential utility in the production of flexible, light-weight, and low-cost large-area devices through roll-to-roll printing *via* solution processing.[1–9] Although the maximum power conversion efficiency (PCE) of the PSCs has been over 10% for single junction solar cells,[10] it still can't meet the demand of commercialization. Generally, in a typical bulk heterojunction (BHJ) PSC, the active layer consists of an interpenetrating network formed by an electron-donor material blended with an electron-acceptor fullerene derivative (typically [6,6]-phenyl-$C_{61}$-butyric acid methyl ester ($PC_{61}BM$) or [6,6]-phenyl-$C_{71}$-butyric acid methyl ester ($PC_{71}BM$)).[11,12] Currently, the most critical challenge in developing ideal electron-donor materials is to design and synthesize conjugated polymers that simultaneously possess broad and strong absorption band in visible and near-infrared region, high hole mobility, suitable energy levels, good solubility for solution processing, optimal morphology and nanoscale phase separation of the interpenetrating network of the donor/acceptor blend active layer.[13]

Conjugated polymers based on thieno[3,4-*b*]thiophene (TT) have been studied extensively as low optical band-gap polymers.[14–16] However, compared with other donor–acceptor (D–A) polymers, the polymers based TT as A building block usually exhibit a lower open circuit voltage ($V_{OC}$), which is the limiting factor for the device's PCE. Various electron-withdrawing groups such as ester (COOR),[17–20] ketone (COR),[21–23] sulfonyl ($SO_2R$),[24–26] fluorine (F),[27,28] trifluoromethyl group ($CF_3$),[29] *N*-alkyl-2,7-dithia-5-azacyclopenta[*a*]pentalene-4,6-dione (DTPD)[30] have been introduced on the 2 or 3 position of TT to tune the highest occupied molecular orbital (HOMO) level to improve $V_{OC}$.

Moreover, there are only several literatures investigated alkylthio-substituent conjugated polymers so far.[31–37] In contrast with alkyl chains, alkylthio substituents are of particular interest for several reasons. First, the van der Waals radius of sulfur (~0.18 nm) is less than that of $-CH_2$ (~0.20 nm), which will reduce the steric strain slightly.[31] Secondly, the sulfur atom is known to be a weak electron donor due to the poor overlap of its orbital with the π-system on the polymer backbone, which will decrease the HOMO and lowest unoccupied molecular orbital (LUMO) levels of the polymer.[33,37] For example, according to the previous report,[33] poly[(3-hexyl-thio)thiophene] (P3HST) showed a lower optical band gap of 1.82 eV compared with poly(3-hexylthiophene) (P3HT, 1.85 eV), and the alkylthio side chains decreased the HOMO energy level of the

[a]*CAS Key Laboratory of Bio-based Materials, Qingdao Institute of Bioenergy and Bioprocess Technology, Chinese Academy of Sciences, Qingdao 266101, China. E-mail: yangrq@qibebt.ac.cn*

[b]*University of Chinese Academy of Sciences, Beijing 100049, China*

[c]*State Key Laboratory of Luminescent Materials and Devices, South China University of Technology, Guangzhou 510641, China*

polymer. However, most alkylthio side chains reported were substituted on the D unit of the D–A type conjugated polymers in the form of thioether. Moreover, a potential problem may exist that sulfur atom in thioether compound can be oxidized easily, which may result in an unpredictable effect to the polymer.

Based on the above consideration, we replaced the alkyl chain of ketone-substituted TT with alkylthio side chain to develop a new acceptor *S*-alkyl thieno[3,4-*b*]thiophene-2-carbothioate (TTS). To our knowledge, the thioester substituent on the acceptor unit has not been reported. Apart from broadening the optical absorption and decreasing the HOMO energy level as previously mentioned, the antioxidant capacity of sulfur atom of thioester can be enhanced. In addition, compared with the TT-based acceptors mentioned previously, it is easier to synthesize monomer TTS, and the homologous polymers obtained exhibit promising photovoltaic performance. In this work, we reported the synthesis and characterization of two new polymers PBDTT-TTSO and PBDTT-TTSE, which consisted of benzodithiophene (BDT) and TTS moieties substituted with octyl or 2-ethylhexyl groups, respectively. Both polymers utilize light absorption to exceed 800 nm. Meanwhile, the two polymers show favorably aligned HOMO and LUMO energy levels relative to that of conventional fullerene acceptors. The photovoltaic performance of PBDTT-TTSE devices display a $V_{OC}$ of 0.70 V, a short circuit current density ($J_{SC}$) of 14.6 mA cm$^{-2}$, a fill factor (FF) of 56.7%, and a PCE of 5.80%. This work demonstrates that the new thioester-substituted acceptor TT moiety is a promising building block for high performance PSCs.

## Results and discussion

### Monomers and polymers synthesis

The synthetic routes for monomers and polymers are shown in Scheme 1.[38,39] Firstly, 3,4-dibromothiophene was monolithiated by *n*-BuLi and subsequently quenched with dimethylformamide (DMF) to produce compound **2** in 82% yield. Then a mixture of compound **2**, ethyl thioglycolate and potassium carbonate was heated at 80 °C for 12 h with copper(II) oxide nanopowder as the catalyst to provide thieno[3,4-*b*]thiophene-2-carboxylate (**3**) in 54% yield. Compound **3** was brominated with *N*-bromosuccinimide (NBS) at room temperature to give compound **4** in 70% yield. After hydrolysis in the alkali medium, the corresponding TT carboxylic acid was obtained. Finally, the monomer **6** can be obtained by the condensation of the carboxylic acid and the corresponding thioalcohol (RSH).

The polymers PBDTT-TTSO and PBDTT-TTSE were synthesized by Stille coupling reaction with tetrakis-(triphenylphosphine)palladium(0) ($Pd(PPh_3)_4$) as the catalyst. The crude products were precipitated in methanol and collected by filtration. Soxhlet purification afforded the black polymers. Gel permeation chromatography (GPC) analysis using tetrahydrofuran as an eluent provided a number-average molecular weight ($M_n$) of 18.5 kDa with a polydispersity index (PDI) of 2.01 for PBDTT-TTSO and a $M_n$ of 25.3 kDa with a PDI of 1.88 for PBDTT-TTSE, with respect to a polystyrene standard.

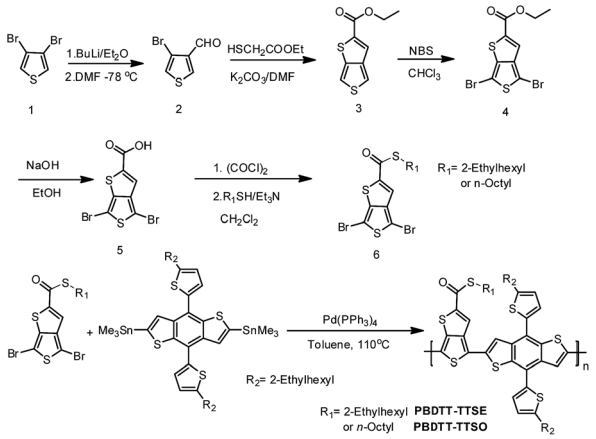


Scheme 1 Synthesis of the monomers and polymers.

### Thermal properties

The thermal properties of the polymers were examined by thermogravimetric analysis (TGA) and the TGA curves are shown in Fig. 1. In the TGA measurement, the decomposition temperatures ($T_d$) at a 5% weight loss occurred under a nitrogen atmosphere are as high as 374 °C and 380 °C for PBDTT-TTSO and PBDTT-TTSE, respectively, which show good thermal stabilities. It is adequate for the fabrication of PSCs and other optoelectronic devices.

### Optical properties

The ultraviolet-visible (UV-vis) absorption spectra of the polymers PBDTT-TTSO and PBDTT-TTSE in dilute chloroform solution and as thin films are shown in Fig. 2. The optical properties of the polymers are listed in Table 1. Both polymers show very similar optical characteristics, covering a broad absorption range from 300 nm to 800 nm. The absorption peaks at short wavelength are originated from π–π* transition of the polymer main chains and side chains, while the absorption peaks at long wavelength could be attributed to the strong intramolecular charge transfer (ICT) between the electron-rich moieties and electron-deficient segments in the polymer

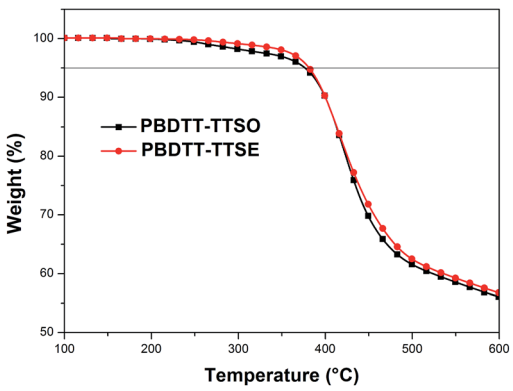


Fig. 1 TGA plots of PBDTT-TTSO and PBDTT-TTSE with a heating rate of 10 °C min$^{-1}$ under the protection of nitrogen.

backbones.[40,41] The absorption peak of the polymer PBDTT-TTSO has a red shift of 19 nm as thin film compared to the absorption peak of 644 nm in dilute chloroform solution. Meanwhile, PBDTT-TTSE shows the absorption peak at 661 nm and an enhanced band at 712 nm in solid film, which indicates slightly increased π–π stacking. The absorption edges of PBDTT-TTSO and PBDTT-TTSE are at 816 and 827 nm corresponding to the optical band gaps of 1.52 and 1.50 eV, respectively. The optical band gaps are lower than those of ester or ketone-substituted polymer PBDTTT-E-T (1.58 eV) and PBDTTT-C-T (1.58 eV).[22] The results also support the viewpoint that the alkylthio side chain can broaden the optical absorption mentioned previously.[33,34,36]

## Electrochemical properties

Electrochemical cyclic voltammetry (CV) was carried out to measure the molecular energy levels of the polymers.[42] The redox potentials are estimated from the onsets of the oxidation and reduction. All voltammograms were calibrated using the ferrocene/ferrocenium ($Fc/Fc^+$) redox couple as the standard, and their energy levels are assumed at −4.8 eV relative to vacuum. The potential of this internal standard under the same condition was 0.39 eV *versus* saturated calomel electrode (SCE). As shown in Fig. 3a, the onsets of oxidation and reduction of PBDTT-TTSO are observed at +0.92 and −0.70 V *vs.* SCE. The corresponding HOMO and LUMO energy levels are estimated to be −5.33 and −3.71 eV according to the empirical equation: $E_{HOMO/LUMO} = -(E_{ox/red} + 4.41)$ eV. Similarly, the HOMO and LUMO energy levels of PBDTT-TTSE are determined to be −5.36 and −3.73 eV (Table 1). The HOMO energy levels of PBDTT-TTSO and PBDTT-TTSE calculated from CV curves are similar to that of DTPD-based polymers PEBDTPD (−5.37 eV).[30] Although the branched side chain can slightly decrease the HOMO level compared to the linear side chain in accordance with that of ester or DTPD-substituted polymers reported,[17,30] the energy levels of both polymers are in the ideal range for the high PCEs according to Brabec's estimation if taking the LUMO energy level of $PC_{71}BM$ as −4.1 eV (Fig. 3b).[43] As well known, the $V_{OC}$ is mainly dependent on the difference between the HOMO energy level of the donor and the LUMO energy level of the fullerene acceptor, the relatively deep-lying HOMO levels of two polymers could give a high $V_{OC}$ in solar cells.

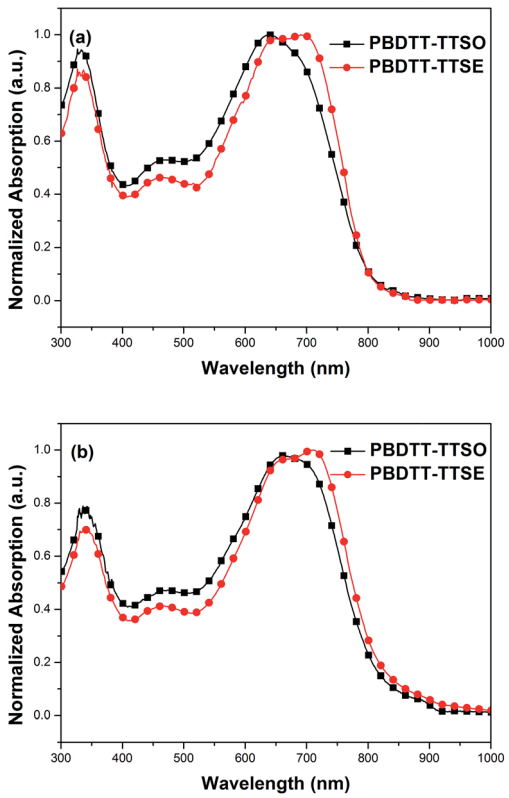


Fig. 2 UV-vis absorption spectra of PBDTT-TTSO and PBDTT-TTSE in dilute chloroform solution (a) and in the film (b).

## Photovoltaic performance

In order to investigate the potential applications of both polymers in solar cells, the BHJ-PSCs were fabricated with device structure of ITO/PEDOT:PSS/polymer:PCBM/Ca/Al, where PEDOT:PSS and Ca layers were employed as buffer layers to facilitate hole and electron extractions. The devices were tested under the illumination of AM 1.5G, 100 mW $cm^{-2}$. The current density–voltage curves of the polymer/$PC_{71}BM$ devices are shown in Fig. 4a and the optimized photovoltaic performance with 1,8-diiodooctane (DIO, 3%, v/v) are listed in Table 2. The device based on PBDTT-TTSO/$PC_{61}BM$ (1 : 1.5, w/w) exhibits a $V_{OC}$ of 0.67 V, a $J_{SC}$ of 11.8 mA $cm^{-2}$ and a FF of 54.7%, yielding a PCE of 4.33%. When replacing $PC_{61}BM$ with $PC_{71}BM$, the $J_{SC}$ can increase to 12.7 mA $cm^{-2}$ while the $V_{OC}$ and FF almost remain unchanged. In comparison, the $V_{OC}$ of PBDTT-TTSE device is ~0.02 V higher than that of PBDTT-TTSO, which is well consistent with their HOMO energy levels (−5.33 eV and −5.36 eV, respectively) (Table 1). The optimized photovoltaic performance of PBDTT-TTSE/$PC_{71}BM$ demonstrates a $V_{OC}$ of 0.70 V, a $J_{SC}$ of 14.6 mA $cm^{-2}$, a FF of 56.7%, and a PCE of 5.80%, which is almost the same as that of non-fluorine substituted TT-based polymers including ester-substituted polymer PBDTTT-E-T

Table 1 The optical and electrochemical properties of the two polymers

| Polymers | Solution $\lambda_{max}$ (nm) | Film $\lambda_{max}$ (nm) | Film $\lambda_{onset}$ (nm) | $E_g^{opta}$ (eV) | HOMO (eV) | LUMO (eV) | $E_g^{cv}$ (eV) |
|---|---|---|---|---|---|---|---|
| PBDTT-TTSO | 644 | 663 | 816 | 1.52 | −5.33 | −3.71 | 1.62 |
| PBDTT-TTSE | 642, 702 | 661, 712 | 827 | 1.50 | −5.36 | −3.73 | 1.63 |

[a] Estimated from the onset wavelength of the optical absorption: $E_g^{opt} = 1240/\lambda_{onset}$.

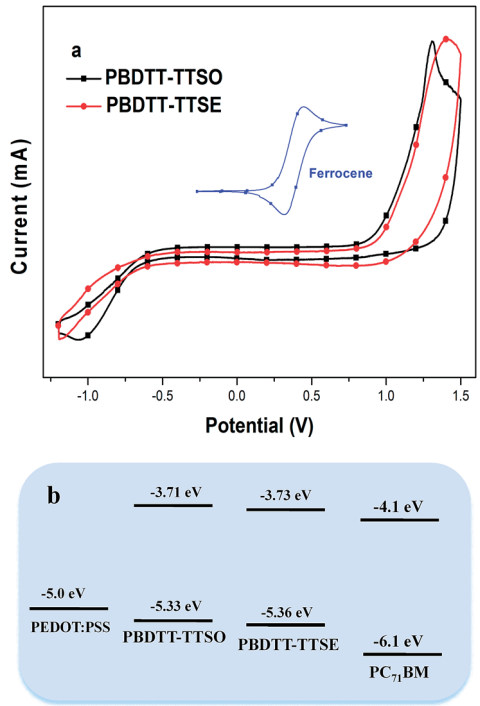


Fig. 3 (a) Cyclic voltammograms of both films and ferrocene in a 0.1 mol $L^{-1}$ $n$-$Bu_4NPF_6$ acetonitrile solution at a sweep rate of 100 mV $s^{-1}$ and (b) energy level diagram for the polymers used in this work.

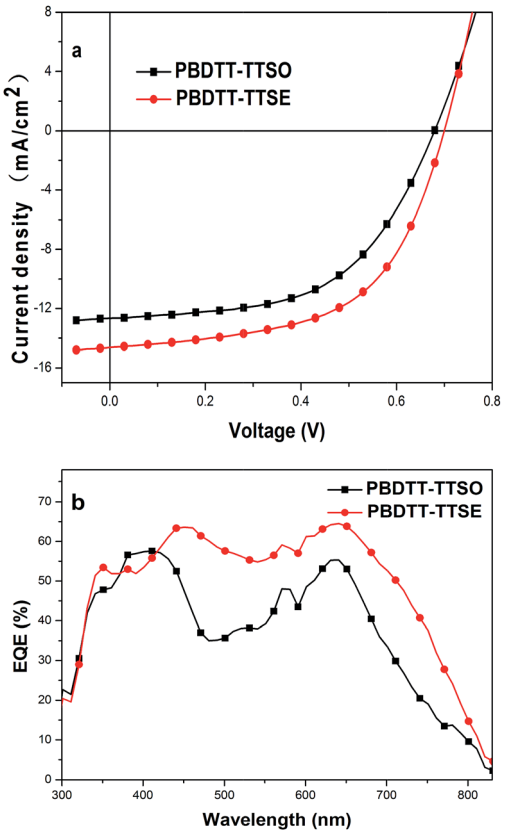


Fig. 4 (a) The $J$–$V$ curves and (b) EQE spectra of the PSCs based on polymer : $PC_{71}BM$ (1 : 1.5) with 3% DIO (v/v).

Table 2 Photovoltaic properties of PSCs based on polymers : PCBM = 1 : 1.5 (w/w) with 3%DIO (v/v)

| Polymers | $V_{OC}$ (V) | $J_{SC}$ (mA $cm^{-2}$) | FF (%) | PCE (%) | Hole mobility ($cm^2$ $V^{-1}$ $s^{-1}$) |
|---|---|---|---|---|---|
| PBDTT-TTSO[a] | 0.67 | 11.8 | 54.7 | 4.33 | — |
| PBDTT-TTSO[b] | 0.68 | 12.7 | 54.6 | 4.70 | $4.75 \times 10^{-5}$ |
| PBDTT-TTSE[a] | 0.70 | 12.6 | 57.5 | 5.03 | — |
| PBDTT-TTSE[b] | 0.70 | 14.6 | 56.7 | 5.80 | $1.38 \times 10^{-4}$ |

[a] $PC_{61}BM$ as the acceptor. [b] $PC_{71}BM$ as the acceptor.

(6.21%),[22] DTPD-based polymers PEBDTPD (5.30%),[30] and sulfonyl-based polymers PBDTTT-S-T (5.93%).[26]

EQE spectra were measured under illumination of monochromatic light shown in Fig. 4b. The EQE curves of the devices show a good photo response in the 300–800 nm regions, which coincides with the corresponding absorption spectra. It is observed that the EQE value of PBDTT-TTSE is higher than that of PBDTT-TTSO in the range (430–800 nm). The highest value for PBDTT-TTSE can exceed 60% at 460 and 650 nm. The result agrees well with the higher $J_{SC}$ and PCE of PBDTT-TTSE than PBDTT-TTSO.

The hole mobilities of the polymers were investigated by the space charge limited current (SCLC) method. High mobility could guarantee effective charge carrier transport to the electrodes and reduce the photocurrent loss in photovoltaic devices. The hole only mobilities of the blend films were measured with a device structure of ITO/PEDOT:PSS/polymer:$PC_{71}BM$ (100 nm)/Au. The SCLC model is described by

$$J_{SCLC} = \frac{9}{8}\varepsilon_0\varepsilon_r\mu\frac{V^2}{L^3} \quad (1)$$

here, $J$ stands for current density, $\varepsilon_0$ is the permittivity of free space, $\varepsilon_r$ is the relative dielectric constant of the transport medium, $\mu$ is the hole mobility, $V$ is the internal potential in the device and $L$ is the thickness of the active layer. The internal potential $V$ is obtained by subtracting the built-in voltage ($V_{bi}$) and the voltage drop ($V_s$) from the series resistance of the substrate from the applied voltage ($V_{appl}$), accordingly: $V = V_{appl} - V_{bi} - V_s$. The relationship between current and voltage in the hole-only devices of polymer films is shown in Fig. 5 and the calculated hole mobilities of polymers are listed in Table 2. The hole mobility of PBDTT-TTSO is determined at $4.75 \times 10^{-5}$ $cm^2$ $V^{-1}$ $s^{-1}$ while the hole mobility of PBDTT-TTSE film is three times as that of PBDTT-TTSO, which can reach $1.38 \times 10^{-4}$ $cm^2$ $V^{-1}$ $s^{-1}$. The high mobility of PBDTT-TTSE is in favor of the charge carrier transport and could result in high current density, which is consistent with the $J_{SC}$ data of PSC devices in Table 2. The relatively lower mobility may be one reason of low photovoltaic performance compared to those of ester or ketone-substituted polymer PBDTTT-E-T ($6.74 \times 10^{-3}$ $cm^2$ $V^{-1}$ $s^{-1}$) and PBDTTT-C-T (0.27 $cm^2$ $V^{-1}$ $s^{-1}$).

## Morphological characterization

Atomic force microscopy (AFM) was employed to investigate the surface morphology of the blend films of polymer/$PC_{71}BM$

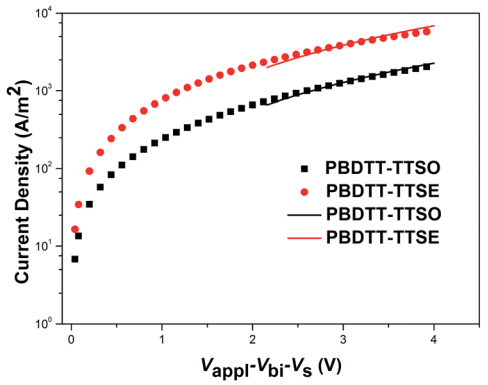


Fig. 5 *J–V* characteristics of the device ITO/PEDOT:PSS/polymer:$PC_{71}BM$ (100 nm)/Au. The symbols are experimental data for the transport of holes, and the solid lines are fitted according to SCLC model.

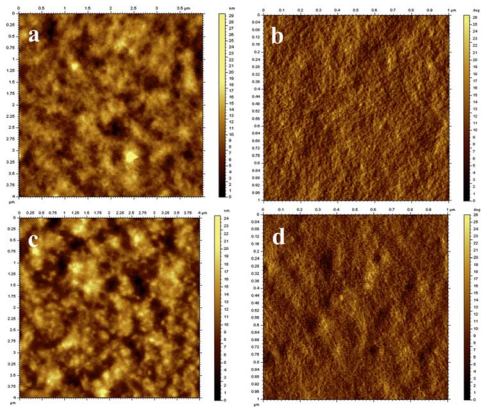


Fig. 6 AFM height (a, c, 4 μm × 4 μm) and phase images (b, d, 1 μm × 1 μm) of polymer: $PC_{71}BM$ (1 : 1.5) blend films: (a and b) PBDTT-TTSO, (c and d) PBDTT-TTSE, respectively.

(1 : 1.5, w/w) with the addictive of 3% DIO.[44] The height and phase images are shown in Fig. 6 and the preparation conditions are the same as the device fabrication. AFM images of both blend films exhibit smooth surfaces while the root-mean-squared (RMS) roughness of the PBDTT-TTSO/$PC_{71}BM$ film (RMS = 2.64 nm) was slightly lower than that of the PBDTT-TTSE/$PC_{71}BM$ film (RMS = 3.13 nm). For the phase image, the dark-colored and light-colored areas correspond to $PC_{71}BM$ domains and polymers, respectively. As we know the exiton diffusion length is less than 20 nm and the perfect domain size should not exceed 30 nm.[45] It can be observed from Fig. 6b and d that the phase images of the blend films exhibit nanoscale phase separation with suitable domain sizes, which could contribute to charge carrier transport and collection. Interesting, the polymer PBDTT-TTSE shows a more desirable nanoscale phase separation with the domain sizes of ~20 nm compared to PBDTT-TTSO. The results are in accord with the photovoltaic performance of the two polymers.

# Experimental section

## Materials

All starting materials and reagents were purchased from commercial sources and used without further purification, unless otherwise mentioned. Toluene was distilled over sodium in the presence of benzophenone as indicator. $CHCl_3$ and $CH_2Cl_2$ were distilled over calcium hydride.

## Instrumentation

$^1H$ and $^{13}C$ NMR spectra were measured on a Bruker Advance III 600 spectrometer with tetramethylsilane (TMS, $\delta = 0$ ppm) as an internal standard. GPC analyses were made using tetrahydrofuran (THF) as eluant and polystyrene standard as reference. UV-vis absorption spectra were performed on Lambda25 spectrophotometer. Cyclic voltammetry (CV) measurements were taken on a CHI660D electrochemical workstation. The CV experiments were carried out at room temperature with a conventional three-electrode system using a glassy carbon electrode as working electrode, Pt wire as the counter electrode, and saturated calomel electrode as the reference electrode. Tetrabutylammonium phosphorus hexafluoride ($Bu_4NPF_6$, 0.1 M) in acetonitrile solution was used as the supporting electrolyte, and the scan rate was 100 mV $s^{-1}$. Ferrocene/ferrocenium ($Fc/Fc^+$) was used as the internal standard. Thermal gravimetric analysis (TGA) measurements were performed on STA-409 at a heating rate of 10 °C $min^{-1}$. Topographic images of the active layers were obtained through atomic force microscopy (AFM) in tapping mode under ambient conditions using an Agilent 5400 instrument.

## Photovoltaic device fabrication

The PSCs devices were fabricated with a configuration of ITO/PEDOT:PSS/polymers:PCBM/Ca/Al. A thin layer of PEDOT:PSS [30 nm, Baytron PVP AI 4083] was spin-cast on precleaned ITO-coated glass at 4000 rpm. After baking at 150 °C for 20 min, the substrates were transferred into glovebox, where the active layer (~100 nm) of the blend of the polymer and PCBM was spin-coated on the PEDOT:PSS layer. Finally, a Ca (10 nm)/Al (100 nm) metal top electrode was thermal evaporated onto the active layer under about $2 \times 10^{-4}$ Pa. The active area of the device was 0.1 $cm^2$ defined by shadow mask. The current density–voltage (*J–V*) characteristics were measured with a Keithley 2420 source measurement unit under simulated 100 mW $cm^{-2}$ (AM 1.5G) irradiation from a Newport solar simulator. Light intensity was calibrated with a standard silicon solar cell. The external quantum efficiencies (EQE) of solar cells were analyzed using a certified Newport incident photon conversion efficiency measurement system.

## Monomer synthesis

**4-Bromothiophene-3-carbaldehyde (2).** To a solution of 3,4-dibromothophene (7.74 g, 32.0 mmol) in diethyl ether, *n*-BuLi (32.0 mmol, 20 mL, 1.6 M in hexane) was added dropwise at −78 °C and stirred for 40 min. Then DMF (2.33 g, 32.0 mmol) was

 

added. The solution was stirred for 2 h followed by quenching of the reaction with saturated $NH_4Cl$. The reaction mixture was extracted twice with ether and the combined organic layers were dried over anhydrous $Na_2SO_4$. After concentration, the residue was purified by column chromatography to give the product as pale yellow oil in 82% yield. $^1$H NMR (600 MHz, $CDCl_3$), $\delta$ (ppm): 9.94 (s, 1H), 8.16 (d, $J = 3.6$ Hz, 1H), 7.37 (d, $J = 3.6$ Hz, 1H). $^{13}$C NMR (150 MHz, $CDCl_3$), $\delta$ (ppm): 184.7, 137.4, 134.6, 125.0, 111.3.

**Ethyl thieno[3,4-*b*]thiophene-2-carboxylate (3).** A mixture of 4-bromothiophene-3-carbaldehyde (1.0 g, 5.23 mmol), ethylmercapto acetate (0.69 g, 5.75 mmol), CuO nanopowder (85 mg), and $K_2CO_3$ (1.08 g, 7.85 mmol) in DMF was heated at 80 °C for 12 h. After the mixture was cooled to room temperature, it was poured into ice-water and extracted twice with ether. The combined organic layers were washed with water and brine successively and dried over $Na_2SO_4$. After concentration, the residue was purified by column chromatography to give the product as yellow solid in 54% yield. $^1$H NMR (600 MHz, $CDCl_3$), $\delta$ (ppm): 7.70 (s, 1H), 7.59 (d, $J = 3.0$ Hz, 1H), 7.28 (d, $J = 3.0$ Hz, 1H), 4.37 (q, $J = 7.2$ Hz, 2H), 1.39 (t, $J = 7.2$ Hz, 3H). $^{13}$C NMR (150 MHz, $CDCl_3$), $\delta$ (ppm): 163.2, 145.9, 139.83, 139.82, 123.5, 116.6, 111.3, 61.7, 14.4.

**Ethyl 2,5-dibromothieno[3,4-*b*]thiophene-2-carboxylate (4).** To a solution of compound **3** (3.5 g, 16.5 mmol) in chloroform (30 mL) was added NBS (7.4 g, 41.3 mmol). And then the reactant was stirred for 3 h at room temperature, followed by addition of water (100 mL). After extraction with chloroform, the organic phase was washed with water, dried over $Na_2SO_4$. After concentration, the residue was purified by column chromatography to give the product as yellow solid in 72% yield. $^1$H NMR (600 MHz, $CDCl_3$), $\delta$ (ppm): 7.54 (s, 1H), 4.38 (q, $J = 7.2$ Hz, 2H), 1.40 (t, $J = 7.2$ Hz, 3H). $^{13}$C NMR (150 MHz, $CDCl_3$), $\delta$ (ppm): 162.3, 145.6, 141.1, 140.4, 123.3, 102.2, 97.1, 62.1, 14.1.

**4,6-Dibromothieno[3,4-*b*]thiophene-2-carboxylic acid (5).** A mixture of compound **4** (4 g, 10.8 mmol) and NaOH (0.86 g, 22 mmol) in ethanol (100 mL) was refluxed overnight. After cooling to room temperature, the reaction mixture was poured into 100 mL water and extracted with petroleum. Then, the water phase was acidified with concentrated HCl. A yellow solid was collected by filtration, and then crystallized from ethanol to yield the product as yellow solid in 90% yield. $^1$HNMR (600 MHz, DMSO-$d_6$), $\delta$ (ppm): 13.87 (brs, 1H), 7.53 (s, 1H).

**General synthesis of monomers (6).** In a 100 mL flask, to a solution of compound **5** (3 mmol) in $CH_2Cl_2$ was added oxalyl chloride (0.5 mL) at 0 °C. After stirring overnight, the reactant was concentrated under pressure to give yellow solid without any purification for next step. To the solution of corresponding thioalcohol (3 mmol) and $Et_3N$ (6 mmol) was added the solution of the above acyl chloride in $CH_2Cl_2$ at 0 °C. And the reactant continued to stir for 12 h. After concentration, the residue was purified by column chromatography to give target product.

*S*-Octyl 4,6-dibromothieno[3,4-*b*]thiophene-2-carbothioate (TTSO), pale yellow solid, yield: 53%. $^1$H NMR (600 MHz, $CDCl_3$), $\delta$ (ppm): 7.52 (s, 1H), 3.09 (q, $J = 7.2$ Hz, 2H), 1.70–1.65 (m, 2H), 1.44–1.39 (m, 2H), 1.36–1.15 (m, 8H), 0.88 (t, $J = 7.2$ Hz, 3H). $^{13}$C NMR (150 MHz, $CDCl_3$), $\delta$ (ppm): 185.7, 148.7, 145.5, 139.8, 120.6, 103.2, 97.3, 32.8, 29.6, 29.4, 29.2, 29.1, 28.9, 22.6, 14.1.

*S*-(2-Ethylhexyl) 4,6-dibromothieno[3,4-*b*]thiophene-2-carbothioate (TTSE), oil, yield: 58%. $^1$H NMR (600 MHz, $CDCl_3$), $\delta$ (ppm): 7.53 (s, 1H), 3.17–3.11 (m, 2H), 1.64–1.59 (m, 1H), 1.45–1.26 (m, 8H), 0.94–0.87 (m, 6H). $^{13}$C NMR (150 MHz, $CDCl_3$), $\delta$ (ppm): 185.7, 148.7, 145.6, 139.6, 120.5, 103.0, 97.4, 39.3, 33.5, 32.6, 28.9, 25.9, 22.9, 14.1, 10.9.

**Polymer synthesis**

*General method of polymerization.* Bis(trimethyltin) BDT monomer (0.20 mmol), compound **6** (0.20 mmol) were mixed in 4 mL toluene and 1 mL DMF. After being purged with argon for 15 min, Pd $(PPh_3)_4$ (11.5 mg) was added as the catalyst, and the mixture was then purged with argon for another 25 min. The reaction mixture was refluxed for 24 h. Then the reaction mixture was cooled to room temperature, and the polymer was precipitated by addition of 50 mL methanol, filtered through a Soxhlet thimble. The precipitate was then subjected to Soxhlet extraction with methanol, hexane and chloroform. The polymer was recovered as solid from the chloroform fraction by precipitation from methanol. The black solid was dried under vacuum to afford the titled polymer.

PBDTT-TTSO, black solid, yield: 87%, $^1$H NMR (600 MHz, $CDCl_3$), $\delta$ (ppm): 8.06–6.69 (m, 7H), 3.41–2.66 (m, 6H), 2.01–1.22 (m, 30H), 1.15–0.76 (m, 15H).

PBDTT-TTSE, black solid, yield: 93%, $^1$H NMR (600 MHz, $CDCl_3$), $\delta$ (ppm): 8.13–6.63 (m, 7H), 3.63–2.65 (m, 6H), 1.97–1.22 (m, 27H), 1.19–0.73 (m, 18H).

## Conclusion

In summary, we replaced the alkyl chain of ketone-substituted thieno[3,4-*b*]thiophene with alkylthio side chain to develop a new acceptor thioester-based acceptor (TTS), which was synthesized easily. Then, two new polymers PBDTT-TTSO and PBDTT-TTSE were designed and synthesized by Stille coupling reaction. The TTS acceptor moieties made the two polymers exhibit a lower band gap (~1.5 eV) and desirable HOMO and LUMO energy levels relative to the fullerene acceptors for PSCs. The PBDTT-TTSE-based photovoltaic device demonstrates a $V_{OC}$ of 0.70 V, a $J_{SC}$ of 14.6 mA cm$^{-2}$, a FF of 56.7%, and a high PCE of 5.80%. This study indicates that thioester substituted thieno[3,4-*b*]thiophene may be a highly useful building block for further design of high performance photovoltaic polymers.

## Acknowledgements

The authors are deeply grateful to the National Natural Science Foundation of China (21202181, 21274161, 51173199, 61107090), the Ministry of Science and Technology of China (2014CB643501, 2010DFA52310), and Qingdao Municipal Science and Technology Program (11-2-4-22-hz) for financial support.

## Notes and references

1 G. Yu, J. Gao, J. C. Hummelen, F. Wudl and A. J. Heeger, *Science*, 1995, **270**, 1789–1791.

2 P. M. Beaujuge and J. M. Frechet, *J. Am. Chem. Soc.*, 2011, **133**, 20009–20029.
3 H. J. Son, B. Carsten, I. H. Jung and L. Yu, *Energy Environ. Sci.*, 2012, **5**, 8158–8170.
4 P.-L. T. Boudreault, A. Najari and M. Leclerc, *Chem. Mater.*, 2011, **23**, 456–469.
5 D. Zhu and R. Yang, *J. Nano Energy Power Res.*, 2013, **2**, 73–91.
6 P.-L. T. Boudreault, S. Beaupré and M. Leclerc, *Polym. Chem.*, 2010, **1**, 127–136.
7 J.-T. Chen and C.-S. Hsu, *Polym. Chem.*, 2011, **2**, 2707–2722.
8 X. Zhan and D. Zhu, *Polym. Chem.*, 2010, **1**, 409–419.
9 H.-L. Yip and A. K. Y. Jen, *Energy Environ. Sci.*, 2012, **5**, 5994–6011.
10 Y. Liu, J. Zhao, Z. Li, C. Mu, W. Ma, H. Hu, K. Jiang, H. Lin, H. Ade and H. Yan, *Nat. Commun.*, 2014, **5**, 5293.
11 C. Winder and N. S. Sariciftci, *J. Mater. Chem.*, 2004, **14**, 1077–1086.
12 C.-Z. Li, H.-L. Yip and A. K. Y. Jen, *J. Mater. Chem.*, 2012, **22**, 4161–4177.
13 Y. Li, *Acc. Chem. Res.*, 2012, **45**, 723–733.
14 Y. Liang and L. Yu, *Acc. Chem. Res.*, 2010, **43**, 1227–1236.
15 L. Huo and J. Hou, *Polym. Chem.*, 2011, **2**, 2453–2461.
16 J. M. Szarko, B. S. Rolczynski, S. J. Lou, T. Xu, J. Strzalka, T. J. Marks, L. Yu and L. X. Chen, *Adv. Funct. Mater.*, 2014, **24**, 10–26.
17 Y. Liang, D. Feng, Y. Wu, S.-T. Tsai, L. Gang, C. Ray and L. Yu, *J. Am. Chem. Soc.*, 2009, **131**, 7792–7799.
18 Y. Liang, Y. Wu, D. Feng, S.-T. Tsai, H.-J. Son, L. Gang and L. Yu, *J. Am. Chem. Soc.*, 2009, **131**, 56–57.
19 Y. Liang, Z. Xu, J. Xia, S. T. Tsai, Y. Wu, G. Li, C. Ray and L. Yu, *Adv. Mater.*, 2010, **22**, E135–E138.
20 Q. Xu, F. Wang, D. Qian, Z. Tan, L. Li, S. Li, X. Tu, G. Sun, X. Hou, J. Hou and Y. Li, *ACS Appl. Mater. Interfaces*, 2013, **5**, 6591–6597.
21 J. Hou, H.-Y. Chen, S. Zhang, R. I. Chen, Y. Yang, Y. Wu and G. Li, *J. Am. Chem. Soc.*, 2009, **131**, 15586–15587.
22 L. Huo, S. Zhang, X. Guo, F. Xu, Y. Li and J. Hou, *Angew. Chem., Int. Ed.*, 2011, **50**, 9697–9702.
23 Z.-G. Zhang, H. Li, Z. Qi, Z. Jin, G. Liu, J. Hou, Y. Li and J. Wang, *Appl. Phys. Lett.*, 2013, **102**, 143902.
24 Y. Huang, L. Huo, S. Zhang, X. Guo, C. C. Han, Y. Li and J. Hou, *Chem. Commun.*, 2011, **47**, 8904–8906.
25 Y. Huang, X. Guo, F. Liu, L. Huo, Y. Chen, T. P. Russell, C. C. Han, Y. Li and J. Hou, *Adv. Mater.*, 2012, **24**, 3383–3389.
26 Y. Wu, Z. Li, W. Ma, Y. Huang, L. Huo, X. Guo, M. Zhang, H. Ade and J. Hou, *Adv. Mater.*, 2013, **25**, 3449–3455.
27 M. Zhang, X. Guo, S. Zhang and J. Hou, *Adv. Mater.*, 2014, **26**, 1118–1123.
28 M. Zhang, X. Guo, W. Ma, S. Zhang, L. Huo, H. Ade and J. Hou, *Adv. Mater.*, 2014, **26**, 2089–2095.
29 P. Deng, Z. Wu, K. Cao, Q. Zhang, B. Sun and S. R. Marder, *Polym. Chem.*, 2013, **4**, 5275–5282.
30 S.-O. Kim, Y.-S. Kim, H.-J. Yun, I. Kang, Y. Yoon, N. Shin, H. J. Son, H. Kim, M. J. Ko, B. Kim, K. Kim, Y.-H. Kim and S.-K. Kwon, *Macromolecules*, 2013, **46**, 3861–3869.
31 J. A. Schneider, A. Dadvand, W. Wen and D. F. Perepichka, *Macromolecules*, 2013, **46**, 9231–9239.
32 C. Cui, W.-Y. Wong and Y. Li, *Energy Environ. Sci.*, 2014, **7**, 2276–2284.
33 L. Huo, Y. Zhou and Y. Li, *Macromol. Rapid Commun.*, 2009, **30**, 925–931.
34 L. Ye, S. Zhang, W. Zhao, H. Yao and J. Hou, *Chem. Mater.*, 2014, **26**, 3603–3605.
35 D. Ouyang, M. Xiao, D. Zhu, W. Zhu, Z. Du, N. Wang, Y. Zhou, X. Bao and R. Yang, *Polym. Chem.*, 2015, **6**, 55–63.
36 D. Lee, E. Hubijar, G. J. D. Kalaw and J. P. Ferraris, *Chem. Mater.*, 2012, **24**, 2534–2540.
37 D. Lee, S. W. Stone and J. P. Ferraris, *Chem. Commun.*, 2011, **47**, 10987–10989.
38 M.-J. Baek, S.-H. Lee, K. Zong and Y.-S. Lee, *Synth. Met.*, 2010, **160**, 1197–1203.
39 J. H. Park, Y. G. Seo, D. H. Yoon, Y.-S. Lee, S.-H. Lee, M. Pyo and K. Zong, *Eur. Polym. J.*, 2010, **46**, 1790–1795.
40 J. Zhang, W. Cai, F. Huang, E. Wang, C. Zhong, S. Liu, M. Wang, C. Duan, T. Yang and Y. Cao, *Macromolecules*, 2011, **44**, 894–901.
41 E. Zhou, J. Cong, K. Tajima and K. Hashimoto, *Chem. Mater.*, 2010, **22**, 4890–4895.
42 Y. Li, Y. Cao, J. Gao, D. Wang, G. Yu and A. J. Heeger, *Synth. Met.*, 1999, **99**, 243–248.
43 M. C. Scharber, D. Mühlbacher, M. Koppe, P. Denk, C. Waldauf, A. J. Heeger and C. J. Brabec, *Adv. Mater.*, 2006, **18**, 789–794.
44 M. Campoy-Quiles, T. Ferenczi, T. Agostinelli, P. G. Etchegoin, Y. Kim, T. D. Anthopoulos, P. N. Stavrinou, D. D. C. Bradley and J. Nelson, *Nat. Mater.*, 2008, **7**, 158–164.
45 M. Drees, H. Hoppe, C. Winder, H. Neugebauer, N. S. Sariciftci, W. Schwinger, F. Schäffler, C. Topf, M. C. Scharber, Z. Zhu and R. Gaudiana, *J. Mater. Chem.*, 2005, **15**, 5158.

 